Extended Abstracts of the 2020 International Conference on Solid State Devices and Materials, VIRTUAL conference, 2020, pp49-50

A-5-05 (Late News)

TCAD Simulation of Phonon Thermal Transport in a Semiconductor Device

Junichi Hattori, Tsutomu Ikegami, and Koichi Fukuda
National Institute of Advanced Industrial Science and Technology (AIST), Tsukuba, Ibaraki 305-8568, Japan
Phone: +81-29-861-3121, E-mail: j.hattori@aist.go.jp

Abstract—We consider a method to simulate phonon thermal transport in a semiconductor device together with charge carrier transport in the framework of technology computer-aided design (TCAD) simulation. This method enables us to treat each phonon mode separately. We implement it in our own TCAD simulator and demonstrate the simulation of heat generation and transport in a transistor having a thin silicon-on-insulator body.

1. Introduction

In designing the thermal behavior of integrated circuits, it is essential to understand the generation and transport of heat in their components such as transistors, for which simulation is highly useful. The simulation of heat transport is generally conducted with the heat equation derived from Fourier's law. Although the law requires that heat carriers have a mean free path sufficiently shorter than the dimensions of their medium, this requirement is not fulfilled in modern deeply scaled semiconductor devices. In order to accurately predict the heat transport in such devices, it is necessary to simulate the transport of heat carriers themselves, namely phonons. The phonon transport can be described by the Boltzmann equation, and various formulations and their solutions have been proposed [1–6]. In the simulations based on them except for particle methods [5, 6], the transport of charge carriers, namely electrons and holes, was ignored; consequently, their interaction with phonons was not sufficiently taken into account. The electron and hole transport is typically simulated with a technology computer-aided design (TCAD) simulator based on a finite volume method in order to predict the electrical behavior of semiconductor devices in industry practices. In this study, we consider a method of simulating the phonon transport together with the electron and hole transport in the TCAD simulation framework to improve TCAD simulators' capability of predicting the thermal behavior of deeply scaled semiconductor devices.

2. Governing Equation

The Boltzmann equation for phonons can be written as

$$\frac{\partial f_{n\boldsymbol{k}}}{\partial t} + \boldsymbol{v}_{n\boldsymbol{k}} \cdot \nabla f_{n\boldsymbol{k}} + \frac{f_{n\boldsymbol{k}} - f^{\mathrm{e}}_{n\boldsymbol{k}}}{\tau_{n\boldsymbol{k}}} - g_{n\boldsymbol{k}} = 0, \tag{1}$$

where $f_{n\boldsymbol{k}}$ is the number density of phonons of the mode located at wavevector $\boldsymbol{k}$ on the nth branch in a dispersion relation and $f^{\mathrm{e}}_{n\boldsymbol{k}}$ is its value in an equilibrium state. Also, $\boldsymbol{v}_{n\boldsymbol{k}}$ is the phonon group velocity, $\tau_{n\boldsymbol{k}}$ the relaxation time, and $g_{n\boldsymbol{k}}$ the generation rate. Rewriting Eq. (1) for the density of energy carried by phonons and then introducing the difference from its value in the equilibrium state of a reference temperature T^{r}, $\varepsilon_{n\boldsymbol{k}}$, we obtain the following equation:

$$\frac{\partial \varepsilon_{n\boldsymbol{k}}}{\partial t} + \boldsymbol{v}_{n\boldsymbol{k}} \cdot \nabla \varepsilon_{n\boldsymbol{k}} + \frac{\varepsilon_{n\boldsymbol{k}} - c_{n\boldsymbol{k}}(T - T^{\mathrm{r}})}{\tau_{n\boldsymbol{k}}} - \hbar\omega_{n\boldsymbol{k}} g_{n\boldsymbol{k}} = 0. \tag{2}$$

Here, $\omega_{n\boldsymbol{k}}$ is the phonon angular frequency, $c_{n\boldsymbol{k}} = \hbar\omega_{n\boldsymbol{k}} \partial f_{n\boldsymbol{k}} / \partial T$ the heat capacity, and T the local temperature defined as

$$T = T^{\mathrm{r}} + \left(\sum_{n,\boldsymbol{k}} \varepsilon_{n\boldsymbol{k}} \Big/ \sum_{n,\boldsymbol{k}} c_{n\boldsymbol{k}} \right). \tag{3}$$

In a semiconductor, electrons and holes affect phonons through $g_{n\boldsymbol{k}}$, which was assumed to be given by

$$\hbar\omega_{n\boldsymbol{k}} g_{n\boldsymbol{k}} = \left[\boldsymbol{J} \cdot \boldsymbol{E} + (R - G)(E_{\mathrm{g}} + 3k_{\mathrm{B}}T) \right] \Big/ \sum_{n,\boldsymbol{k}} 1. \tag{4}$$

Here, the first term of the right-hand side, the dot product of the current density $\boldsymbol{J}$ and the electric field $\boldsymbol{E}$, represents the Joule heating. The second term represents the heating and cooling due to the nonradiative recombination and generation of electron–hole pairs, R and G denote the recombination and generation rates, and E_{g} is the band gap energy. Also, the energy change of the phonon system by these mechanisms was assumed to be evenly distributed to each mode. On the other hand, phonons affect electrons and holes through the temperature dependence of their mobility and E_{g}. Solving an equation in the standard TCAD simulation framework requires its form discretized by a finite volume method, that is, by integrating it over a finite volume surrounding a node of a computational mesh, which volume is referred to as a control volume (CV). We incorporated Eqs. (2) and (3) into our homemade TCAD, Impulse TCAD [7, 8], which automates part of the equation discretization.

3. Boundary Conditions

We solved Eq. (2) not only for the nodes inside a phonon medium but also for those on its boundary. In the discretization of Eq. (2), the integral of the second term in the left-hand side over a CV can be rewritten as an integral over the CV's faces. We expressed the boundary condition of Eq. (2) by changing the value $A^{\mathrm{b}}_{n\boldsymbol{k}}$ of the integral over the faces forming part of the boundary. The simplest boundary is one with a heat bath, where phonons are in an equilibrium state. When the temperature of the heat bath is T^{b}, for an outgoing mode, $A^{\mathrm{b}}_{n\boldsymbol{k}} = c_{n\boldsymbol{k}}(T^{\mathrm{b}} - T^{\mathrm{r}})\boldsymbol{v}_{n\boldsymbol{k}} \cdot \boldsymbol{S}^{\mathrm{b}}$ with $\boldsymbol{S}^{\mathrm{b}}$ being the vector area of the CV's face forming part of the boundary. For an incoming mode, on the other hand, all of the energy carried to the boundary is absorbed into the heat bath and therefore $A^{\mathrm{b}}_{n\boldsymbol{k}} = \varepsilon_{n\boldsymbol{k}}\boldsymbol{v}_{n\boldsymbol{k}} \cdot \boldsymbol{S}^{\mathrm{b}}$.

We simulated the phonon thermal transport in a 1-μm-long Si bar with a square cross section of side length 100 nm whose one

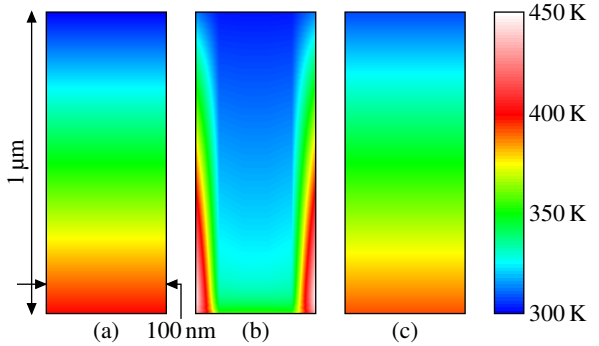

Fig. 1. Temperature distributions in a cross-section of Si square bars calculated from (a) the heat equation and [(b) and (c)] the Boltzmann equation of Eq. (2). Only in (c), a boundary condition that phonons are purely specularly reflected was explicitly applied to the bar sides.

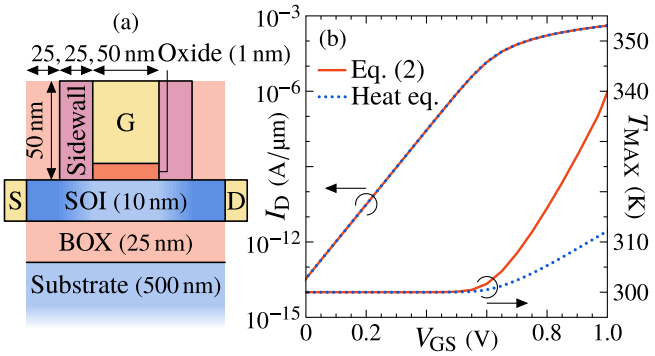

Fig. 2. (a) Schematic of a transistor with an SOI body. (b) Its drain current and maximum temperature in the body as functions of the gate-to-source voltage V_{GS} calculated with (solid lines) or without (dotted lines) taking into account the phonon transport in the body. The drain-to-source voltage was set to 1 V.

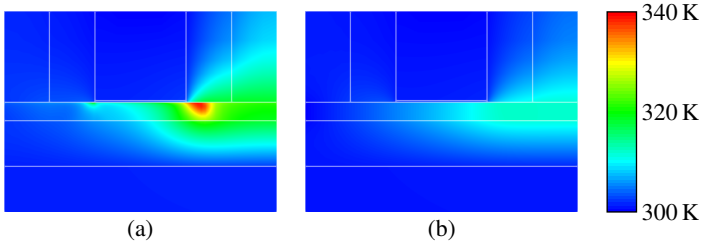

Fig. 3. Temperature distributions in the SOI transistor at a V_{GS} of 1 V simulated (a) with and (b) without taking into account the phonon transport in the SOI body.

end and the other end were respectively connected to heat baths of temperature 300 and 400 K. In the simulation, phonons in the bar were approximated by those in single-crystalline Si, whose properties were obtained from lattice dynamics calculations with the modified valence force field model [9], and 178 modes were considered, which means 178 equations of Eq. (2) were solved simultaneously. Also, the initial T distribution, shown in Fig. 1(a), was obtained from the heat equation. The resulting T distribution is shown in Fig. 1(b). At the center of the hot end, T is obviously lower than the connected heat bath temperature T^{b} of 400 K. The above-mentioned boundary condition cannot control the energy carried by phonons traveling toward or along a boundary. Thus, at the boundary, T does not become equal to T^{b}. On the other hand, unexpected hot regions appear at the bar sides of the hot end side. Since each phonon travels only in the direction of $\boldsymbol{v}_{n\boldsymbol{k}}$, phonons that reach a boundary will not leave it unless a proper condition is set on the boundary.

The bar sides are a form of boundary of a phonon medium with respect to a different material. The energy carried to the boundary by incoming mode phonons is partially transmitted and the rest is carried to the inside by outgoing mode phonons together with the energy transmitted from the outer material. Therefore, $A^{\mathrm{b}}_{n\boldsymbol{k}}$ can be written for an incoming mode i as

$$A^{\mathrm{b}}_i = \varepsilon_i \boldsymbol{v}_i \cdot \boldsymbol{S}^{\mathrm{b}} \tag{5a}$$

and for an outgoing mode o as

$$A^{\mathrm{b}}_o = -\sum_i r_{io}[\varepsilon_i - c_i(T^{\mathrm{b}} - T^{\mathrm{r}})]\boldsymbol{v}_i \cdot \boldsymbol{S}^{\mathrm{b}} - c_o(T^{\mathrm{b}} - T^{\mathrm{r}})\boldsymbol{v}_o \cdot \boldsymbol{S}^{\mathrm{b}}. \tag{5b}$$

Here, r_{io} is the reflectance of i to o, and T^{b} is the temperature at the boundary of the outer material. Figure 1(c) shows the T distribution in the Si bar under the assumption that the phonon energy incident on a bar side is purely specularly reflected. This boundary condition eliminates the unnatural hot regions shown in Fig. 1(b).

4. Simulation

Finally, we simulated the phonon transport together with the electron and hole transport in a metal–oxide–semiconductor field-effect transistor with a 10-nm-thick silicon-on-insulator (SOI) body and a 50-nm-long gate shown in Fig. 2(a). The drain current I_{D} and the maximum temperature in the SOI body T_{MAX} at a drain-to-source voltage of 1 V are shown in Fig. 2(b) as functions of the gate-to-source voltage. In the simulation, the Boltzmann equation of Eq. (2) was solved only for the heat transport in the SOI body while the heat equation was solved for that in the other regions. Also, the boundary of the SOI body with the source electrode was assumed to be connected to a heat bath of temperature 300 K, the boundary with the drain electrode to be purely specular, and the boundaries with the other regions to have a transmittance of 0.5 and a specular reflectance of 0.5. Under the last boundary condition, the interfaces between SOI and oxide have a thermal resistance of $1.518 \times 10^{-9}\ \mathrm{m^2K/W}$, which is in good agreement with the theoretical calculation [10]. Figure 2(b) also shows the results of applying the heat equation to the SOI body. Comparing the two results, we can see that, although I_{D} is almost the same, T_{MAX} is obviously higher when the phonon transport is considered. As can be seen from the temperature distributions shown in Fig. 3, the temperature difference is large near the entrance of the drain region, where strong Joule heating occurs. With the heat equation, heat is transported efficiently along the temperature gradient. On the other hand, heat transport by phonons is less efficient, because phonons have their own traveling directions, which causes a hot spot.

5. Conclusions

We developed a method to simulate thermal transport by phonons together with charge transport by electrons and holes in a form applicable to standard TCAD simulators. Using our homemade TCAD simulator in which this method was implemented, we simulated the heat generation and transport in an SOI transistor as an example. Our simulation method can treat each phonon mode separately and therefore it can connect the atomistic calculation of phonon properties in materials directly to the TCAD simulation of the thermal behavior of semiconductor devices.

Acknowledgment—This work is supported by a Grant-in-Aid for Scientific Research (No. JP20K04611) from JSPS.

References

[1] P. G. Sverdrup *et al.*, J. Heat Transf. **123**, 130 (2001).
[2] J. Y. Murthy and S. R. Mathur, J. Heat Transf. **125**, 904 (2003).
[3] S. V. J. Narumanchi *et al.*, Heat Mass Transf. **42**, 478 (2006).
[4] F. G. VanGessel and P. W. Chung, Comput. Methods. Appl. Mech. Eng. **317**, 1012 (2017).
[5] J. A. Rowlette and K. E. Goodson, IEEE Trans. Electron Devices **55**, 220 (2008).
[6] K. Kukita and Y. Kamakura, J. Appl. Phys. **114**, 154312 (2013).
[7] National Institute of Advanced Industrial Science and Technology (AIST), Impulse TCAD (2020) [https://unit.aist.go.jp/d-tech/en/ImpulseTCAD/].
[8] T. Ikegami *et al.*, J. Comput. Electron. **18**, 534 (2019).
[9] A. Paul *et al.*, J. Comput. Electron. **9**, 160 (2010).
[10] B. Deng *et al.*, J. Appl. Phys. **115**, 084910 (2014).